



Modeling and Optimization of Sisal Fiber Degradation Treatment by Calcined Bentonite for Cement Composite Materials

Tsion Amsalu Fode, Yusufu Abeid Chande Jande & Thomas Kivevele

To cite this article: Tsion Amsalu Fode, Yusufu Abeid Chande Jande & Thomas Kivevele (2024) Modeling and Optimization of Sisal Fiber Degradation Treatment by Calcined Bentonite for Cement Composite Materials, Journal of Natural Fibers, 21:1, 2408632, DOI: [10.1080/15440478.2024.2408632](https://doi.org/10.1080/15440478.2024.2408632)

To link to this article: <https://doi.org/10.1080/15440478.2024.2408632>



© 2024 The Author(s). Published with license by Taylor & Francis Group, LLC.



[View supplementary material](#)



Published online: 06 Oct 2024.



[Submit your article to this journal](#)



Article views: 434



[View related articles](#)



[View Crossmark data](#)



Citing articles: 2 [View citing articles](#)

Modeling and Optimization of Sisal Fiber Degradation Treatment by Calcined Bentonite for Cement Composite Materials

Tsion Amsalu Fode^{a,b,c,d}, Yusufu Abeid Chande Jande^{a,b,c}, and Thomas Kivevele^{a,b}

^aSchool of Materials, Energy, Water, and Environmental Science (MEWES), The Nelson Mandela African Institution of Science and Technology, Arusha, Tanzania; ^bWater Infrastructure and Sustainable Energy Futures (WISE-Futures) Centre of Excellence, The Nelson Mandela African Institution of Science and Technology, Arusha, Tanzania; ^cStructural Material and Engineering Research Group, The Nelson Mandela African Institution of Science and Technology, Arusha, Tanzania; ^dDepartment of Civil Engineering, Wollega University, Nekemte, Ethiopia

ABSTRACT

The treatment of sisal fiber by pozzolanic materials like kaolin and silica-fume has been explored; however, no study has modeled and optimized the effect of sisal fiber degradation treatment using calcined bentonite. Therefore, the present study investigate the effects of treating sisal fiber with different doses of calcined bentonite, bentonite calcination temperatures, and times on fiber breaking load, degradation resistance, and water absorption using the central composite design-response surface method (CCD-RSM). The best performance of the optimum treated sisal fiber selected from the CCD-RSM based on the established goal of maximizing breaking load and degradation resistance with minimum water absorption, it was obtained a calcined bentonite dose of 30.067%, a bentonite calcination temperature of 800°C, and a calcination time of 179.99 min. Based on these factors, experimentally found sisal fiber breaking load 12.87 N, degradation resistance 98.44%, and water absorption 39.05%, all are within the 95% confidence level compared to the optimum numerical suggested values. Hence, the optimum treated sisal fiber improved breaking load by 33.37% and degradation resistance by 98%, while it reduced water absorption by 60.95%, compared to raw sisal fiber. Besides these, the optimum treated sisal fiber exhibits higher surface roughness and lower porosity than the raw sisal fiber.

摘要




已经使用高岭土和硅粉等火山灰材料处理剑麻纤维，但还没有研究模拟和优化煅烧膨润土对剑麻纤维降解处理的效果。因此，本研究采用中心复合设计响应面法（CCD-RSM）研究了不同煅烧膨润土剂量、膨润土煅烧温度和时间处理剑麻纤维对纤维断裂载荷、抗降解性和吸水率的影响。根据实验发现的剑麻纤维断裂载荷为12.87 N，抗降解性为98.44%，吸水率为39.05%，与最佳数值建议值相比，在煅烧膨润土剂量为30.067%、膨润土煅烧温度为800°C、煅烧时间为179.99分钟条件下，从CCD-RSM中选出的最佳处理剑麻纤维的最佳性能在95%的置信水平内。因此，与生剑麻纤维相比，经过最佳处理的剑麻纤维的断裂载荷提高了33.37%，耐降解性提高了98%，吸水率降低了60.95%。除此之外，经过最佳处理的剑麻纤维比生剑麻纤维具有更高的表面粗糙度和更低的孔隙率。

KEYWORDS

Sisal fiber; bentonite; treatment; roughness; water absorption; degradation

关键词

剑麻纤维; 膨润土; 治疗; 粗糙度; 吸水率; 退化; 命名法

CONTACT Tsion Amsalu Fode  fodet@nm-aist.ac.tz; Yusufu Abeid Chande Jande  yusufu.jande@nm-aist.ac.tz  School of Materials, Energy, Water, and Environmental Science (MEWES), The Nelson Mandela African Institution of Science and Technology, P. O. Box 447, Arusha, Tanzania

© 2024 The Author(s). Published with license by Taylor & Francis Group, LLC.

This is an Open Access article distributed under the terms of the Creative Commons Attribution-NonCommercial License (<http://creativecommons.org/licenses/by-nc/4.0/>), which permits unrestricted non-commercial use, distribution, and reproduction in any medium, provided the original work is properly cited. The terms on which this article has been published allow the posting of the Accepted Manuscript in a repository by the author(s) or with their consent.

Introduction

Currently, the world is looking for replacements of construction materials that are eco-friendly and cost-effective. Natural fibers are more beneficial than synthetic fibers due to their greater accessibility, low density, low cost, lower energy consumption, renewability, and carbon-free properties. In addition, in cement composite materials, natural fibers are crucial for reducing shrinkage cracks, enhancing strength and load-carrying capacity, while highly reducing the deformation of cementing materials (Belaadi et al. 2023; Ramesh 2018; Shadrach Jeya Sekaran, Palani Kumar, and Pitchandi 2015). The use of natural fibers in cement composite materials is crucial for withstanding significant stresses and relatively large strain capacity after concrete cracking, improving strength, and forming high bonds with the cement matrix (Naraganti, Mohan Rao Pannem, and Putta 2019; Bolat et al. 2014; Gao et al. 2022; Hanif et al. 2017; Jamshaid et al. 2022; Machaka, Basha, and Elkordi 2014; Zhang et al. 2018). Besides these, the addition of natural fibers in cement composite materials is beneficial for improving tension force resistance, enhancing deformation capacity and toughness with highly modifying the development of cracks (Abbass, Khan, and Mourad 2018; de Lima et al. 2022; Latifi, Biricik, and Mardani Aghabaglou 2022). The use of natural fibers in concrete improves its post-crack strength, increases ductility, and transfers tensile stress across the crack points, significantly reducing crack width. However, the crack width reduction of concrete depends on the amount and the physical properties of the fibers (Afolayan, Wilson, and Zaphaniah 2019; Mudadu et al. 2018; Wu et al. 2016).

Most natural fibers have cellulose, lignin, hemicellulose, pectin, ash, wax, and sugars (Abirami and Sangeetha 2022; Benítez-Guerrero et al. 2017; de Lima et al. 2022; S. R. Ferreira et al. 2017; Jeyapragash, Srinivasan, and Sathiyamurthy 2020; Naveen et al. 2018; Marvila et al. 2021). Cellulose is the main component of natural fibers that participates in improving mechanical properties, controlling crack opening and propagation, and enhancing tensile strength, ductility, and toughness, while allowing high deformation without compromising integrity (Arshad et al. 2020; Iniya and Nirmalkumar 2021; Izquierdo et al. 2017; Kafodya and Okonta 2018; Shadheer Ahamed, Ravichandran, and Krishnaraja 2021). Moreover, the incorporation of natural fibers in cement composite materials significantly reduces the micro-cracks and decreases the porosity of the concrete matrix, highly improving ductility and reducing the brittleness of construction materials (Belaadi et al. 2023; Hasan et al. 2023; Martinelli et al. 2023).

Among various natural fibers, sisal fiber is crucial in cement composite materials due to its cost-effectiveness, ability to improve mechanical properties, and environmentally friendly nature (Yadav et al. 2021; Belaadi et al. 2013; Asim et al. 2020; Zakaria et al. 2017; Zhou, Saini, and Kastiukas 2017; Ferreira, Cruz, and Fangueiro 2018; Thomas and Stalin Jose 2022; Martinelli et al. 2023; Ali-Boucetta et al. 2021). It is the most extensively cultivated and strong natural fiber extracted from the leaves of the *Agave sisalana* plant that is mainly grown in the tropical and subtropical regions of the world (Singh et al. 2022; Ferreira, Cruz, and Fangueiro 2018; Ferreira et al. 2014). Sisal fiber is traditionally used to make rope, twine, and woven fabrics for the production of bags, for the transport of agricultural products, and marine goods (Abirami and Sangeetha 2022). However, currently, most studies are reporting that sisal fiber can totally or partially replace steel fiber in reinforced concrete, which is beneficial for economic, ecological, and upcoming green building technologies in concrete reinforcement (Herrera-Franco, Carrillo, and Li 2020; Kumar and Roy 2018; Messaouda et al. 2023; Tian et al. 2015; Vijayan and Krishnamoorthy 2019; Zhou, Saini, and Kastiukas 2017). However, sisal fiber is highly moisture-sensitive and can deteriorate due to the mineralization of cementing minerals.

Surface treatment of sisal fibers improves deterioration and moisture sensitivity and enhances interfacial adhesion between the fiber surface and the matrix, which can provide higher bond strength, leading to improved mechanical properties of the composite matrix (Gupta et al. 2020). Mostly, surface treatment of sisal fiber with pozzolanic material is a promising treatment, which highly reduces the content of calcium hydroxide that causes deterioration in the fiber matrix and fills the pores of the sisal fibers, which absorb water that causes fiber aging (De Filho, De Andrade Silva, and Dias Toledo Filho 2013; Fode et al. 2024).

Especially, surface treatment of sisal fiber by pozzolanic materials like metakaolin and nano-clay enhances the interface bond of the sisal fiber with the matrix which prevents the degradation of the sisal fiber from alkaline attack, and reduces CH mineralization attack in cement composite materials (Wei and Meyer 2014a). Furthermore, pozzolanic treatment can reduce the high moisture absorption of sisal fibers due to their surface pores, resulting in a more hydrophobic fiber surface (Gonzalez-Lopez et al. 2020).

de Souza Castoldi, de Souza, and de Andrade Silva (2019) and Fidelis et al. (2016) studied on reduction of sisal fiber degradation through surface treatment with different doses of pozzolanic materials in cement, especially using kaolin and silica-fume. However, it is novel to optimize and model the sisal fiber treatment with pozzolanic materials, specifically using calcined bentonite. Hence, to highly improve sisal fiber resistance to moisture sensitivity and its degradation in cementing materials, the present study aimed to experimentally model and optimize the effects of calcined bentonite on the treatment of sisal fiber using a batch mode CCD-RSM, enabling the study to reach the optimum sisal fiber degradation resistance using calcined bentonite having factors like calcined bentonite replacement dose, bentonite calcination temperature, and time. This was evaluated by assessing the improvement in the sisal fiber degradation, either on its strength or moisture sensitivity, while also examining the microstructure and surface roughness of the optimum treated sisal fiber. Generally, the optimum treated sisal fiber can significantly contribute to the effective use of sisal fiber in construction materials to have safe and economical concrete productions in the eco-friendly environment.

Scopes and limitations of the study

The present study has the scope of modeling and optimizing the effects of different calcined bentonite replacement doses, bentonite calcination temperatures, and times on the surface treatment of sisal fiber. This approach seeks to improve the breaking load, degradation resistance, and moisture sensitivity of sisal fiber in the cementing materials using the response surface modeling method, and optimum treated sisal fiber has been compared with the untreated sisal fiber. However, the study has the limitation that have investigated only on one type of sisal fiber, commonly known as the upper grade.

Materials and methods

Materials

The brushed sisal fiber was collected from Korogwe, Tanzania. Also, the raw bentonite was extracted from Arusha, Tanzania. The chemical composition of the raw bentonite and ordinary Portland cement (OPC) CEM I 32.5 R is taken from the same material used in our previous studies (Fode, Abeid, Jande, and Kivevele 2024; Fode, Jande, et al. 2024). The raw bentonite was calcined after grinding the bentonite sample to pass through a 45 μm sieve. Then, 20 different calcined bentonites were used with OPC to form a slurry using distilled water.

Methods

Experimental design using CCD-RSM

In the RSM, there are several designs, which can be applied for modeling and optimization processes. Hence, central composite design (CCD) is the one that indicates a highly accurate significant prediction of the response variables as well as reveals interactive consequences on the independent variables.

It is a full-factorial design having two levels: center points, which indicate the middle factors, and two axial points [43]. The experimental runs (N) have been determined by Equation 1 as [39, 46].

$$N = 2^K + 2K + C_0 \quad (1)$$

where N, C₀, and k are the required experimental runs, center points, and process variables, respectively.

The CCD-RSM in Design Expert Software (Stat-Ease, version 13) finds the interacting effects of three independent sisal fiber treatment variables, involving bentonite dose (A), bentonite calcination temperature (B), and calcination time (C). Independent factors, their ranges, and the response variables are listed in Table 1. Specifically, the rationale behind the bentonite replacement range was taken from previous studies Wei, Meyer, and Meyer (2017) found that using 50% meta-kaolin pozzolanic material by cement weight for sisal fiber treatment improved the degradation resistance of the sisal fiber but highly reduced the interfacial bond of the fiber with the matrix compared to 30% substitution. Also, the lower and upper calcination temperatures and calcination times taken from a previous study indicated that the highest bentonite reactivity occurred at 800°C for 3 h (Cinku, Karakas, and Boylu 2014; Fode, Abeid, Jande, and Kivevele 2024), while dehydration of most clay begins at 200°C (Ali et al. 2012).

Using CCD-RSM, a set of 20 experimental runs statistically generated with varying configurations related to the response variables, y_1 – single fiber breaking load, y_2 – degradation resistance, and y_3 – water absorption, were used for modeling and optimization processes. For all 20 runs, to ensure the authenticity and reliability of the response variables, the measurement was done three times, and the average of the values was recorded, which had six center points, eight factorials, and six axial points of different response variables, as presented in Table 2.

Table 1. Input level of factor variables.

Response factors	Symbol	Units	Level of factor		
			Lower	Middle	Higher
Bentonite dose	A	%	30	7.5	50
Bentonite activation temperature	B	°C	200	500	800
Calcination time	C	Min	120	150	180

Table 2. The actual design value used for all factors with respective space type.

Experimental runs	Space type	Experimental conditions		
		A: Bentonite dose (%)	B: Bentonite activation temperature (°C)	C: Bentonite activation time (min)
Run-1	Center	40.00	500.00	150.00
Run-2	Factorial	30.00	800.00	180.00
Run-3	Factorial	30.00	200.00	120.00
Run-4	Factorial	50.00	800.00	120.00
Run-5	Factorial	30.00	800.00	120.00
Run-6	Axial	53.16	500.00	150.00
Run-7	Axial	40.00	500.00	189.48
Run-8	Factorial	50.00	200.00	120.00
Run-9	Center	40.00	500.00	150.00
Run-10	Axial	26.84	500.00	150.00
Run-11	Axial	40.00	894.82	150.00
Run-12	Center	40.00	500.00	150.00
Run-13	Factorial	30.00	200.00	180.00
Run-14	Axial	40.00	105.18	150.00
Run-15	Center	40.00	500.00	150.00
Run-16	Axial	40.00	500.00	110.52
Run-17	Factorial	50.00	800.00	180.00
Run-18	Center	40.00	500.00	150.00
Run-19	Factorial	50.00	200.00	180.00
Run-20	Center	40.00	500.00	150.00

Sisal fiber surface treatment method

The brushed sisal fiber specified in the materials section was used for treatment. The treatment of the sisal fiber involves a slurry (binder plus water) prepared with different calcined bentonites, as shown in Table 2, conducted separately for all 20 runs. A 30% to 50% different calcined bentonite was used to replace cement to form a binder. Then, by different trials, a fully coated surface of the sisal fiber was obtained at a 0.8 water-to-binder ratio, which was verified through visual inspection. So, the treatment was performed by immersing the sisal fiber in the prepared slurry of each of the 20 runs, and then the sisal fiber was taken out from the slurry and allowed to dry at room temperature. Lastly, as the fibers were not confined or tightly bundled, it was brushed manually twice a week until reaching 28 days, after which all the treated sisal fiber samples taken for durability and mechanical tests evaluation.

Durability and mechanical properties of treated sisal fiber

The different 20 runs of treated sisal fiber were evaluated for single fiber breaking load using the ISTRON tensile strength machine. For each run, tensile strength tests were conducted on six samples, and the average was recorded for each run. The degradation resistance was assessed for the different 20 runs of treated sisal fiber through 10 cycles of wetting and drying in hot water of 75°C, as Wei and Meyer (2014b) found that the degradation of sisal fiber can start significantly in hot water above 70°C. After completing the wetting and drying cycles, tensile strength tests were conducted on six samples for each run, and the average was recorded. Then, the degradation resistance for each run of the treated sisal fiber was calculated, as shown in Equation 2. Additionally, the water absorption of the 20 runs was evaluated by immersing each type of treated sisal fiber in separate water containers at a constant humidity of 20°C for 12 h, as shown in Figure 1. The difference of various weights of the treated sisal fiber before and after entering the water was measured using a digital balance capable of reading to four decimal places. This process was repeated three times for each run, and the average was recorded.

$$Rd = \frac{Ta * 100}{Tb} \quad (2)$$

where Rd is the degradation resistance (%), Ta and Tb are the averages of six single fiber breaking loads, respectively, after and before wetting and dry cycles of sisal fiber degradation.



Figure 1. Water absorption tests for raw and different treated sisal fiber.

Roughness and microstructural properties

The roughness and microstructural properties of sisal fiber are crucial to characterize the interface bond of the fiber and the composite matrix. Therefore, in the present study, the roughness of the raw sisal fiber and the optimum treated sisal fiber, as determined by CCD after experimental validation, was assessed using an atomic force microscope, and the surface microstructures were observed using a scanning electron microscope.

Result and discussion

Building response surface quadratic models

CCD-RSM can evaluate different degrees of models that fit the predicted and actual effects of factors of response variables, as shown in Eq. 3. It can check multiple regression analyses like linear, logarithmic, quadratic, and cubic models and suggest the best fit for the effects of factors on the response. The software used response variables y_1 – single fiber breaking load (N), y_2 – degradation resistance (%), and y_3 – water absorption (%) for different treated sisal fiber with calcined bentonite, as presented in Table 3, to generate the regression model using Eq. 3. As shown in Table 4, the selected model that best fits the effects of factors on breaking load, degradation resistance, and water absorption is the quadratic model. This is due to the P -values of the selected models being significant, while the cubic model is aliased, which indicates that the cubic model is inappropriate.

$$Y = \sigma_0 + \sum_{i=1}^n \sigma_i X_i + \sum_{i=1}^n \sigma_{ii} X_i^2 + \sum_{i=1}^{n-1} \sum_{j=i+1}^n \sigma_{ij} X_i X_j + \varepsilon \quad (3)$$

where Y is the predicted response variable, σ_0 is the constant coefficient, σ_i is the linear coefficient, σ_{ii} is the quadratic coefficient, σ_{ij} is the interaction coefficient, X_i and X_j are the coded values of variables, and ε is the error or unpredicted response variable on the experimental data.

As presented in Table 5, the adequate precisions are 13.9329, 13.3743, and 12.6740, respectively, for breaking load, degradation resistance, and water absorption, which indicate the suggested quadratic model's reliability and appropriateness, having higher values more than 4.00 (Dahish and Almutairi 2023). Also, the percentage coefficient of variance between the predicted and actual values is less than

Table 3. Sisal fiber treatment by calcined bentonite replacement factors of coded form in CCD matrix with response variables value.

Runs	Space type	Factor 1	Factor 2	Factor 3	Response 1	Response 2	Response 3
		A:Bentonite dose (%)	B:Bentonite activation temperature (°C)	C:Bentonite activation time (min)	Sisal fiber breaking load (N)	Degradation resistance (%)	Water absorption (%)
1	Center	0.000	0.000	0.000	11.854	74.49	67.7
2	Factorial	−1.000	1.000	1.000	12.870	98.44	40.71
3	Factorial	−1.000	−1.000	−1.000	10.046	92.57	68.61
4	Factorial	1.000	1.000	−1.000	10.500	55.33	69.96
5	Factorial	−1.000	1.000	−1.000	10.502	70.47	50.67
6	Axial	1.316	0.000	0.000	11.302	48.66	71.39
7	Axial	0.000	0.000	1.316	11.776	77.02	65.53
8	Factorial	1.000	−1.000	−1.000	12.490	42.83	68.85
9	Center	0.000	0.000	0.000	11.623	70.37	63.44
10	Axial	−1.316	0.000	0.000	10.344	91.55	46.08
11	Axial	0.000	1.316	0.000	12.670	87.53	61.47
12	Center	0.000	0.000	0.000	12.865	66.85	75.91
13	Factorial	−1.000	−1.000	1.000	9.368	93.29	58.38
14	Axial	0.000	−1.316	0.000	11.826	88.36	66.44
15	Center	0.000	0.000	0.000	12.172	79.86	74.13
16	Axial	0.000	0.000	−1.316	11.098	59.65	79.01
17	Factorial	1.000	1.000	1.000	12.120	75.25	62.88
18	Center	0.000	0.000	0.000	12.702	85.33	75.91
19	Factorial	1.000	−1.000	1.000	10.896	45.39	65.78
20	Center	0.000	0.000	0.000	12.500	73.28	74.01

Table 4. Fitness summary of various models for treated sisal fiber breaking load, degradation resistance, and water absorption.

Response	Source	Sequential <i>P</i> -value	Lack of fit <i>P</i> -value	Adjusted R^2	Predicted R^2	Remark
Single fiber breaking load	Linear	0.3070	0.0336	0.0460	−0.4291	
	2FI	0.0263	0.0855	0.4091	−0.3219	
	Quadratic	0.0002	0.9967	0.8811	0.8955	Suggested
	Cubic	0.9974	0.6978	0.8060	0.0820	Aliased
Degradation resistance	Linear	0.0001	0.1505	0.6630	0.4977	
	2FI	0.0379	0.3081	0.7783	0.6875	
	Quadratic	0.0139	0.8941	0.8958	0.8362	Suggested
	Cubic	0.8912	0.5006	0.8523	−0.9121	Aliased
Water absorption	Linear	0.0094	0.1278	0.4088	0.2140	
	2FI	0.4884	0.1089	0.3924	−0.4063	
	Quadratic	0.0017	0.8162	0.8154	0.6767	Suggested
	Cubic	0.6638	0.8660	0.7826	0.7268	Aliased

Table 5. Fitness statistical summary for a quadratic model of all responses.

Statistics	Single fiber breaking load	Degradation resistance	Water absorption
Mean	11.58	73.83	65.34
Standard deviation (Std. Dev.)	0.3549	5.36	4.31
Percentage coefficient of variance (C.V%)	3.07	7.27	6.60
Correlation coefficient (R^2)	0.9374	0.9452	0.9029
Predicted R^2	0.8955	0.8362	0.6767
Adjusted R^2	0.8811	0.8958	0.8154
Adequate precision	13.9329	13.3743	12.6740

10%, which shows that the selected quadratic model is reliable. Furthermore, it is observed that the difference between R^2 predicted and adjusted is less than 0.2 for all response variables, which indicates a good prediction of the suggested quadratic models (Boudermine et al. 2024; Dahish and Almutairi 2023; Mohammed et al. 2019).

Analysis of variance for quadratic model response

The ANOVA of the quadratic model is used to identify the significance of the selected model and evaluate the interacting influence of factors on response. Especially, ANOVA can assess the model fitness and significance using *F*- and *P*-values. Hence, as presented in Tables 6–8, ANOVA for the quadratic models of the treated sisal fiber breaking load, degradation resistance, and water absorption indicates that these are significant models having *P*-values less than 0.05, which basically indicates that the chosen factors have influence on the corresponding response variables (Dahish and Almutairi 2023). In addition to these, for the suggested quadratic model to be accurate and reliable, the lack of fit

Table 6. ANOVA of the quadratic model developed for single fiber breaking load of treated sisal fiber.

Sources	Sum of squares	df	Mean square	<i>F</i> -value	<i>P</i> -value	Remark
Model	18.87	9	2.10	16.65	<.0001	Significant
A-Bentonite dose	1.75	1	1.75	13.90	.0039	
B-Bentonite activation temperature	1.61	1	1.61	12.82	.0050	
C-Bentonite activation time	0.5934	1	0.5934	4.71	.0551	
AB	2.79	1	2.79	22.15	.0008	
AC	0.3461	1	0.3461	2.75	.1284	
BC	4.90	1	4.90	38.89	<.0001	
A ²	4.33	1	4.33	34.38	.0002	
B ²	0.0082	1	0.0082	0.0654	.8033	
C ²	1.31	1	1.31	10.41	.0091	
Residual	1.26	10	0.1260			
Lack of Fit	0.0668	5	0.0134	0.0560	.9967	
Pure Error	1.19	5	0.2386	—	—	
Cor Total	20.13	19	—	—	—	

Table 7. ANOVA of the quadratic model developed for degradation resistance of treated sisal fiber.

Sources	Sum of squares	df	Mean square	F-value	P-value	Remark
Model	4960.84	9	551.20	19.16	<.0001	Significant
A-Bentonite dose	3229.57	1	3229.57	112.25	<.0001	
B-Bentonite activation temperature	51.58	1	51.58	1.79	.2102	
C-Bentonite activation time	439.71	1	478.06	16.62	.0022	
AB	439.71	1	439.71	15.28	.0029	
AC	4.82	1	4.82	0.1675	.6909	
BC	248.76	1	248.76	8.65	.0148	
A ²	122.81	1	122.81	4.27	.0657	
B ²	259.42	1	259.42	9.02	.0133	
C ²	189.87	1	189.87	6.60	.0279	
Residual	287.71	10	28.77			
Lack of Fit	66.31	5	13.26	0.2995	.8941	Not significant
Pure Error	221.40	5	44.28			
Cor Total	5248.55	19				

Table 8. ANOVA of the quadratic model developed for water absorption of treated sisal fiber.

Sources	Sum of squares	df	Mean square	F-value	P-value	Remark
Model	1730.41	9	192.27	10.33	.0006	Significant
A-Bentonite dose	592.40	1	592.40	31.82	.0002	
B-Bentonite activation temperature	168.42	1	168.42	9.05	.0132	
C-Bentonite activation time	201.65	1	201.65	10.83	.0081	
AB	142.97	1	142.97	7.68	.0197	
AC	12.60	1	12.60	0.6768	.4299	
BC	1.75	1	1.75	0.0939	.7655	
A ²	373.06	1	373.06	20.04	.0012	
B ²	129.04	1	129.04	6.93	.0250	
C ²	1.72	1	1.72	0.0926	.7672	
Residual	186.18	10	18.62			
Lack of Fit	55.40	5	11.08	0.4236	.8162	Not significant
Pure Error	130.78	5	26.16			
Cor Total	1916.59	19				

(LOF) must not be significant, which is compared to the pure error; hence, the results of the selected quadratic models for all response factors have LOF values more than 0.05, showing that they are not significant and consequently indicating that the suggested models are adaptable (Mohammed et al. 2019).

CCD-RSM diagnostic test towards the developed model

In the response surface method, the significance, adequacy, and accuracy of the selected models can be assessed using diagnostic tests, which have different plots in terms of normal probability curve, DEFIT, and predicted versus actual plots, as shown in Figures 2–4. As illustrated in Figure 2(a–), the normal percentage probability plots, respectively, for external and internal studentized residuals of all runs are confined to the straight line, which indicates for all response factors the error between the actual and predicted values are negligible; hence, the selected quadratic model is accurate and realistic.

Also, as shown in Figure 3(a–), the DFFTTs plot has a line constraint value between -2.12 and $+2.12$, to evaluate the quadratic model selected by the flow of all runs within the limited lines. So, as observed, all the runs of response variables are within the limit, which indicates that the experimental data can affect the anticipated data.

Furthermore, the quadratic model was evaluated by the variation of the actual and predicted data plot, as shown in Figure 4(a–). Hence, as the results indicate for three of the response parameters, all the runs are very near to the straight line of actual vs predicted plots, which shows the accuracy and soundness of the

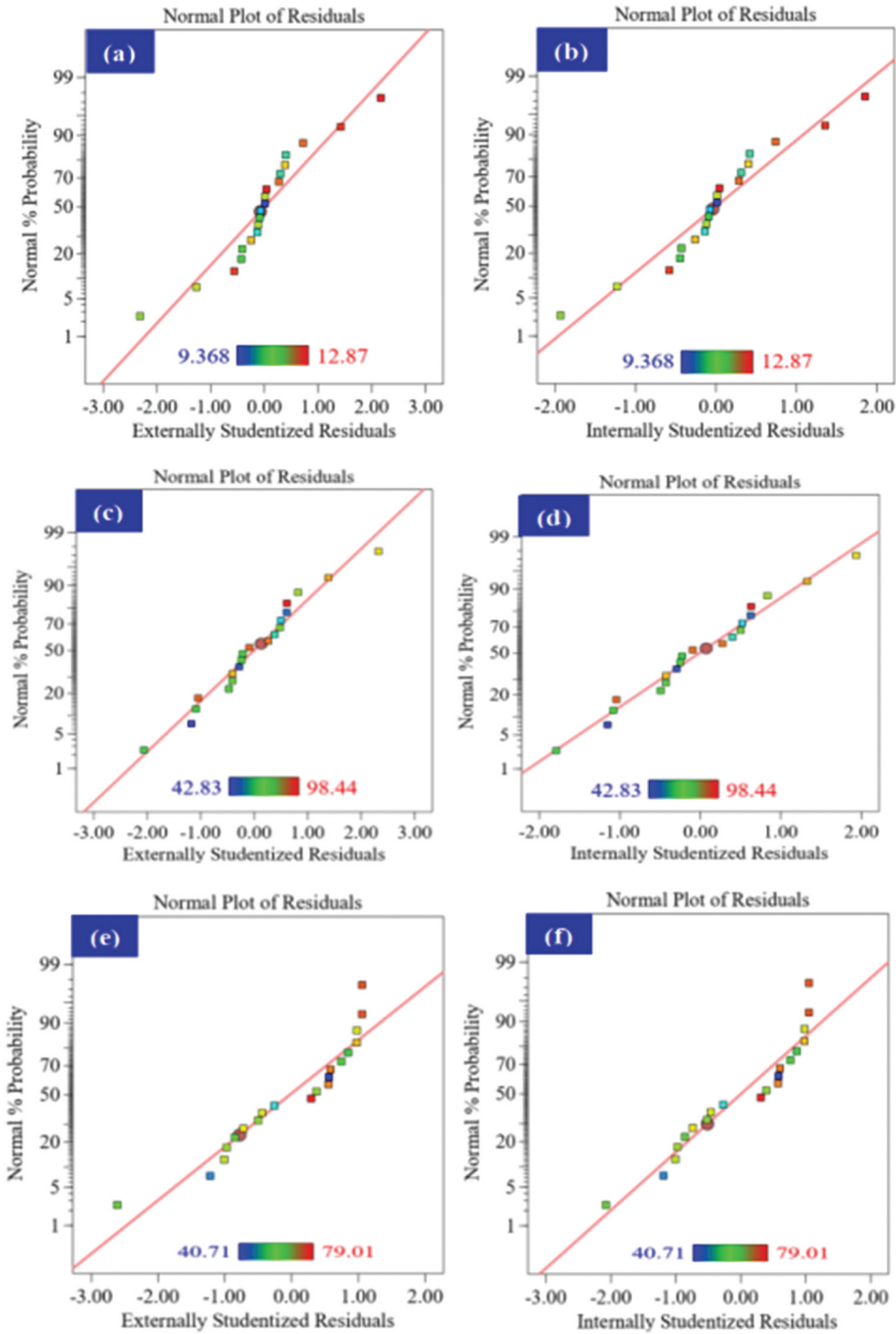


Figure 2. The normal % probability plot vs external and internal studentized residuals, respectively, for (a,b) breaking load, (b,c) degradation resistance, and (c,d) water absorption.

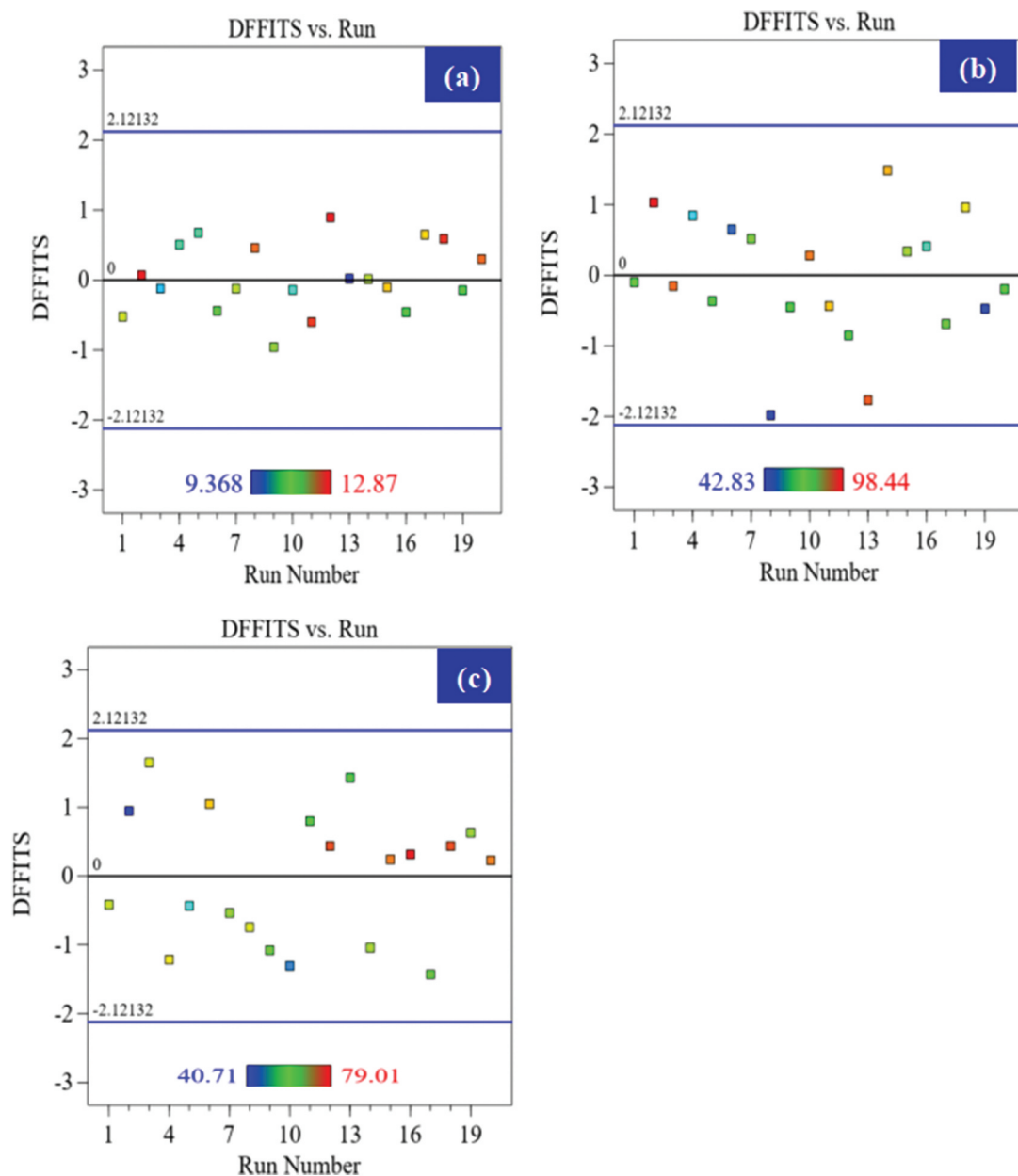


Figure 3. DEFIT plot of sisal fiber treatment response for (a) breaking load, (b) degradation resistance, and (c) water absorption.

selected quadratic models. Also, the other diagnostics tests like residuals vs predicted, residuals vs runs, residuals vs factors, cook distance, Box Cox, and leverage indicate the reliability, fitness, and realism of the quadratic model for all the response variables. Hence, all the diagnostic test results indicate the accuracy of the suggested model, which is consistent with the ANOVA of all the response factors presented in the section of building response surface quadratic models.

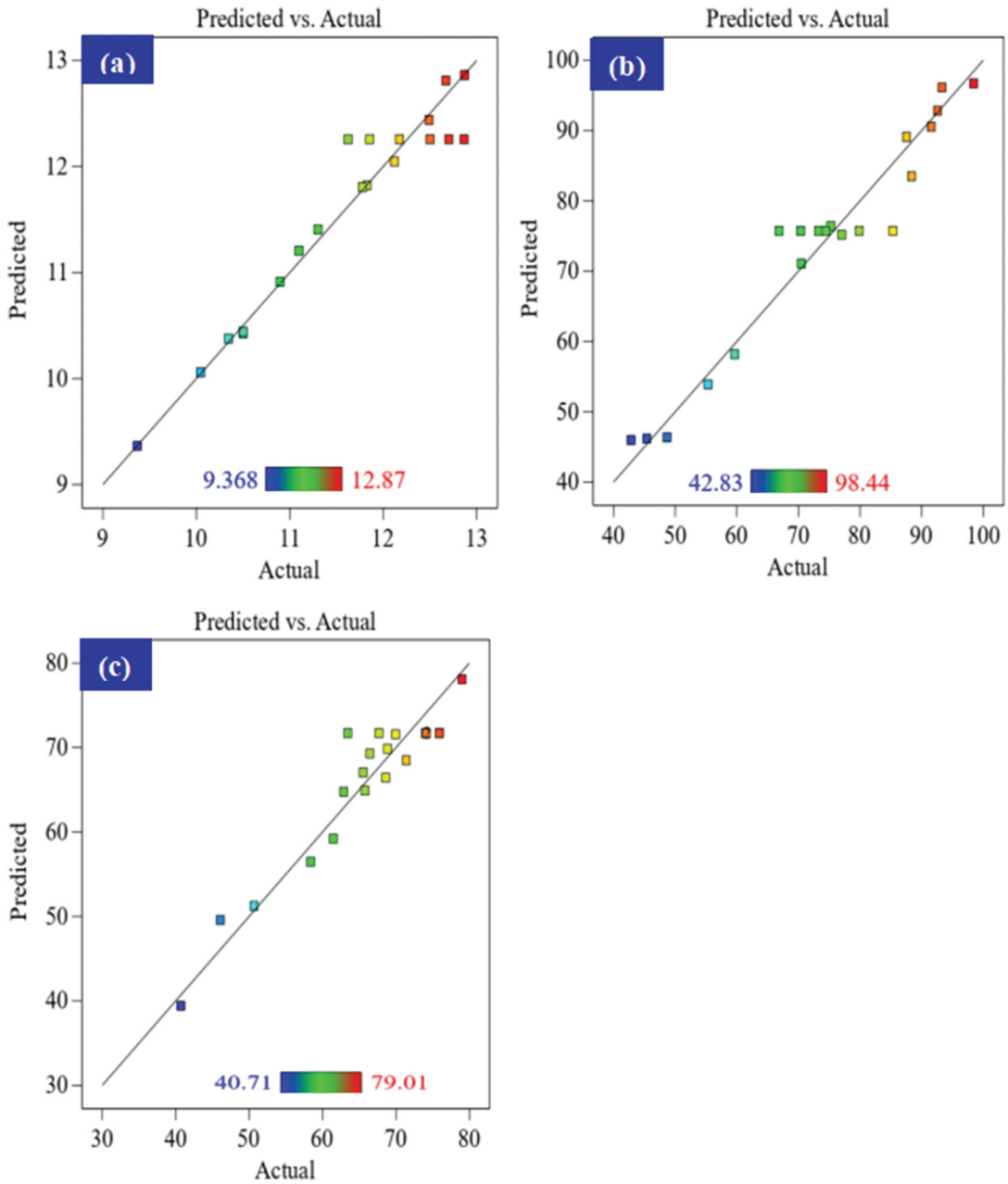


Figure 4. Predicted vs actual plot of sisal fiber treatment response for (a) breaking load, (b) degradation resistance, and (c) water absorption.

Surface modeling by 3D

Single fiber breaking load

The 3D and contour plots of the single fiber breaking load of treated sisal fiber by different calcined bentonites are presented in Figure 5(a–). The result indicates that increasing the calcination temperature and the replacement dose of bentonite used for sisal fiber treatment significantly increases the sisal fiber tensile strength and breaking load. Especially, the highest breaking load was achieved for the

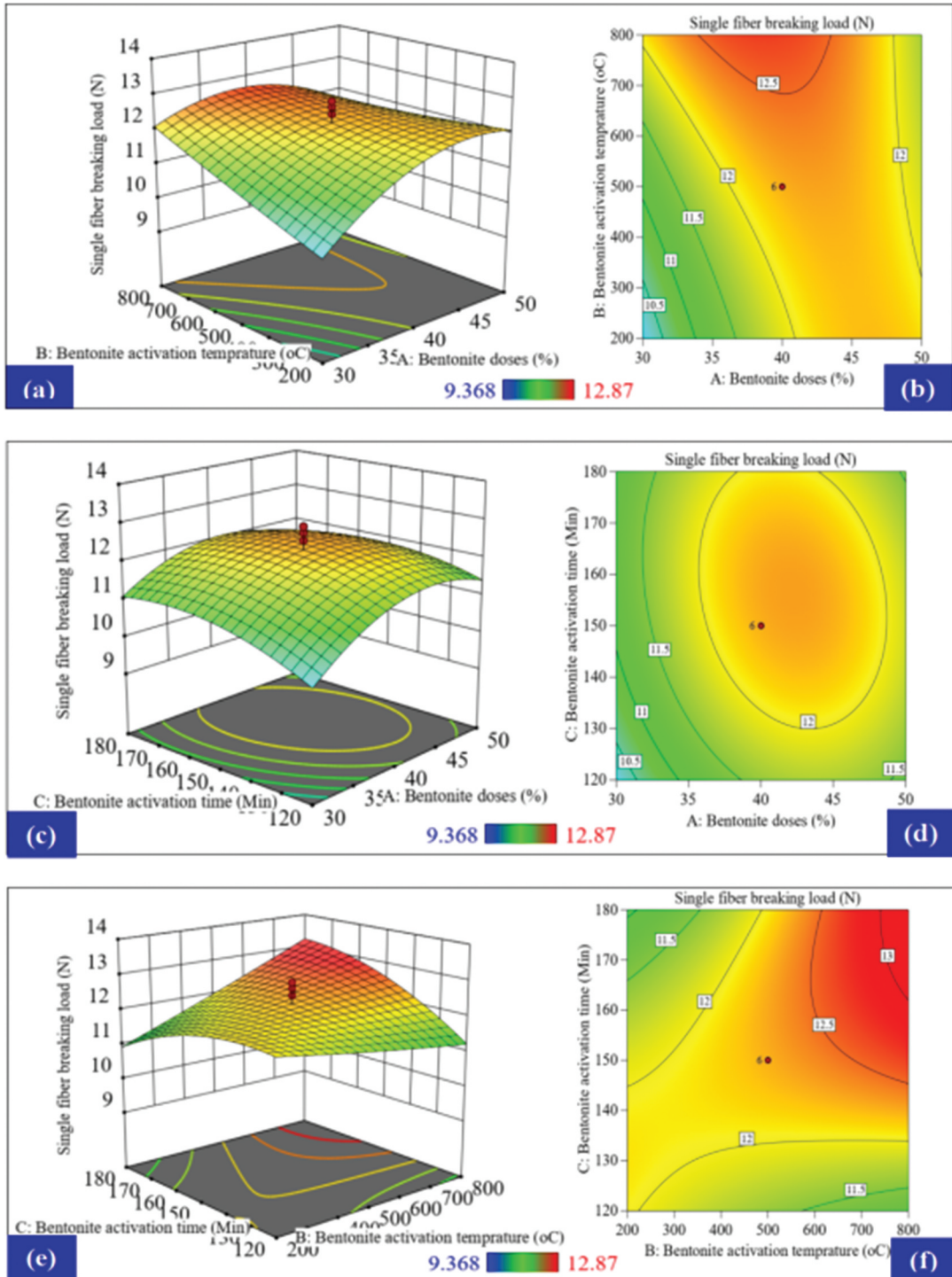


Figure 5. Interaction of treated sisal fiber breaking load with different factors by 3D and contour plots.

treated sisal fiber by 40–45% bentonite replacement at 800°C bentonite calcination temperature. This is because, at higher bentonite calcination temperatures, i.e. near 800°C, bentonite reaches a higher reactivity, which can react with free lime in cement and produce extra calcium silicate hydrate (Fode, Abeid, Jande, and Kivevele 2024; Reddy and Achyutha Kumar Reddy 2021), that can increase the breaking strength of the treated sisal fiber by consuming more free lime in cement and coating the pores of the sisal fiber compared to other samples of treated sisal fiber and also compared to the raw sisal fiber.

Also, as shown in Figure 5(c,d), the breaking load of treated sisal fiber is higher with longer bentonite calcination time and 40–45% calcined bentonite replacement. Reddy and Achyutha Kumar Reddy (2021) found that this is due to the high reactivity of bentonite achieved after 3 h of calcination at 800°C. Additionally, as illustrated in Figure 5(e,f), the highest breaking load of treated sisal fiber was achieved while increasing calcination times from 140–180 min and temperatures of 600–800°C, respectively. Also, at a lower calcination temperature of 200°C for 180 min or at 800°C for 120 min, the breaking load of treated sisal fiber is significantly lower, which indicates that there is minimal reactivity of bentonite at lower calcination temperature or time in which bentonite is mainly found in a consolidated form that needs heating at an optimum temperature (Reddy and Achyutha Kumar Reddy 2021). Consequently, it is used to protect sisal fiber from aging and promise that treated sisal fiber to have a higher breaking load than raw sisal fiber.

Degradation resistance

The 3D and contour plots of the strength of sisal fiber degradation resistance treated with different calcined bentonites are presented in Figure 6(a–). The result indicates that treatment of sisal fiber with higher substitution of calcined bentonite at a low calcination temperature of 200°C yields the lowest degradation resistance compared to the other samples of treated sisal fibers. This is mainly because, at low calcination temperatures, bentonite cannot get higher pozzolanic reactivity, which cannot protect and cover the surface of the sisal fiber tightly. However, increasing bentonite calcination temperatures from 200°C to 800°C and using less than 40% replacement of bentonite used for sisal fiber treatment give higher resistance to the degradation cycles at different wetting and drying conditions, compared to raw sisal fiber and other treated sisal fibers. That is basically while increasing the heating temperature of bentonite activation up to 800°C, it changes from crystalline to amorphous form, which can highly react with the free lime that causes degradation of sisal fiber (Fode, Abeid, Jande, and Kivevele 2024). The present result is similar to the observations of Wei and Meyer (2014a), who found that the substitution of pozzolanic materials like meta-kaolin and nano-clay more than 50% to the cement reduces the capacity of the surface coating of natural pozzolana, consequently decreasing the sisal fiber tensile strength, degradation resistance, and interfacial bond of the fiber with the matrix.

In Figure 6(c,d), at the higher substitution of calcined bentonite, the calcination time of 120 min treated sisal fiber has the lowest degradation resistance. However, increasing the calcination time highly increases the degradation resistance of the treated sisal fiber. This is because, at a lower calcination time, bentonite may not reach its highest reactivity with free calcium hydroxide and may not form a ground cover for the surface of sisal fiber that can protect from degradation. Likewise, as shown in Figure 6(e,f), the degradation resistance of sisal fiber increases with increasing calcination temperature and time of the calcined bentonite. Also, the treated sisal fiber reached the highest aging resistance when calcined for 150–180 min at calcination temperature above 600°C. As Fode, Abeid, Jande, and Kivevele (2024) studied, bentonite reached its highest reactivity and the end of dehydroxylation at 800°C for 3 h, transforme from crystalline to amorphous phase; hence, bentonite can highly react with free calcium hydroxide and protect sisal fiber from mineralization of cement due to free lime.

Water absorption

The 3D and contour plots of the percentage of water absorption for the treated sisal fiber with different calcined bentonites are presented in Figure 7(a–). As the result indicates in Figure 7(a,b), the water

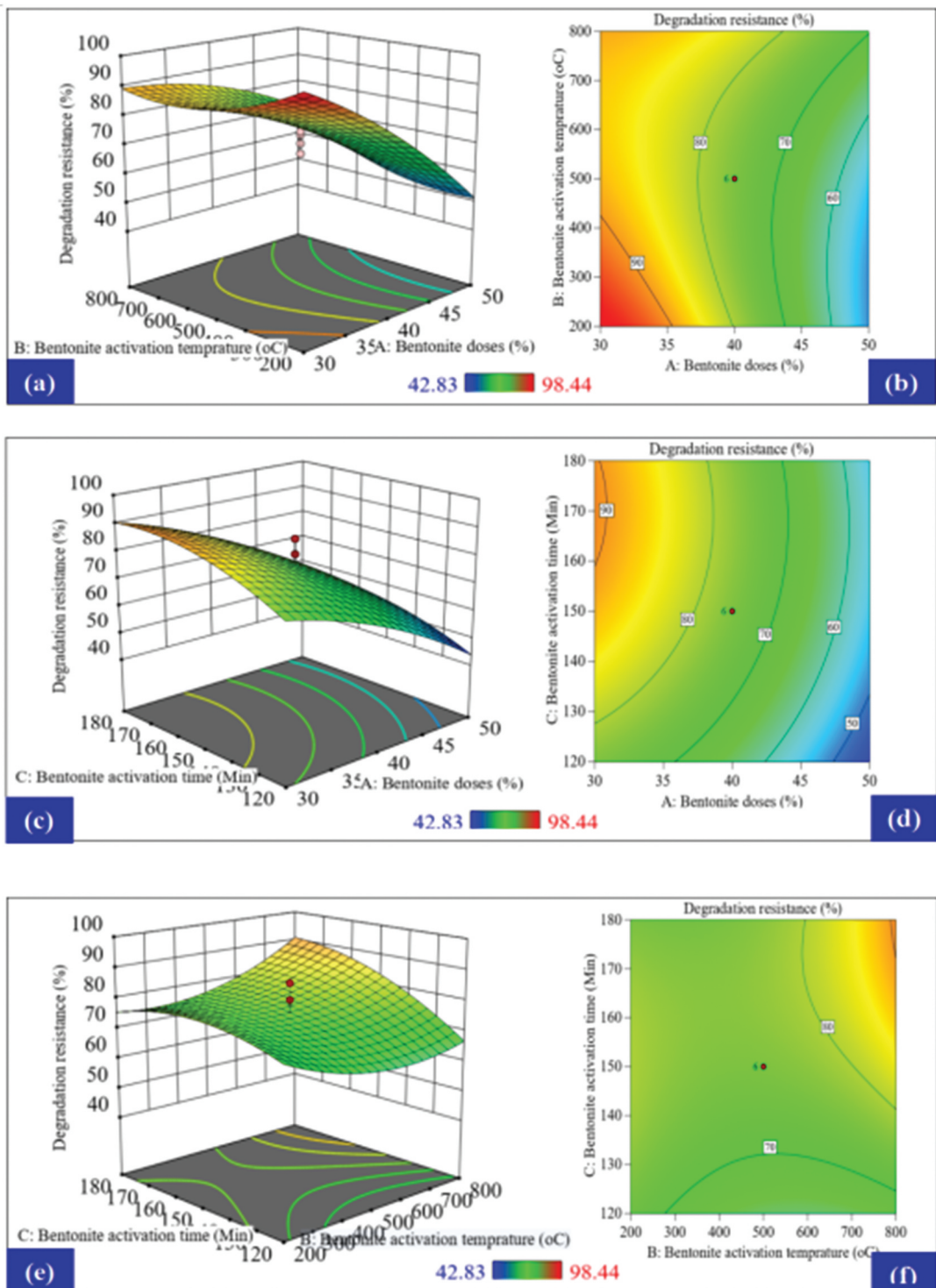


Figure 6. Interaction of treated sisal fiber degradation resistance with different factors by 3D and contour plots.

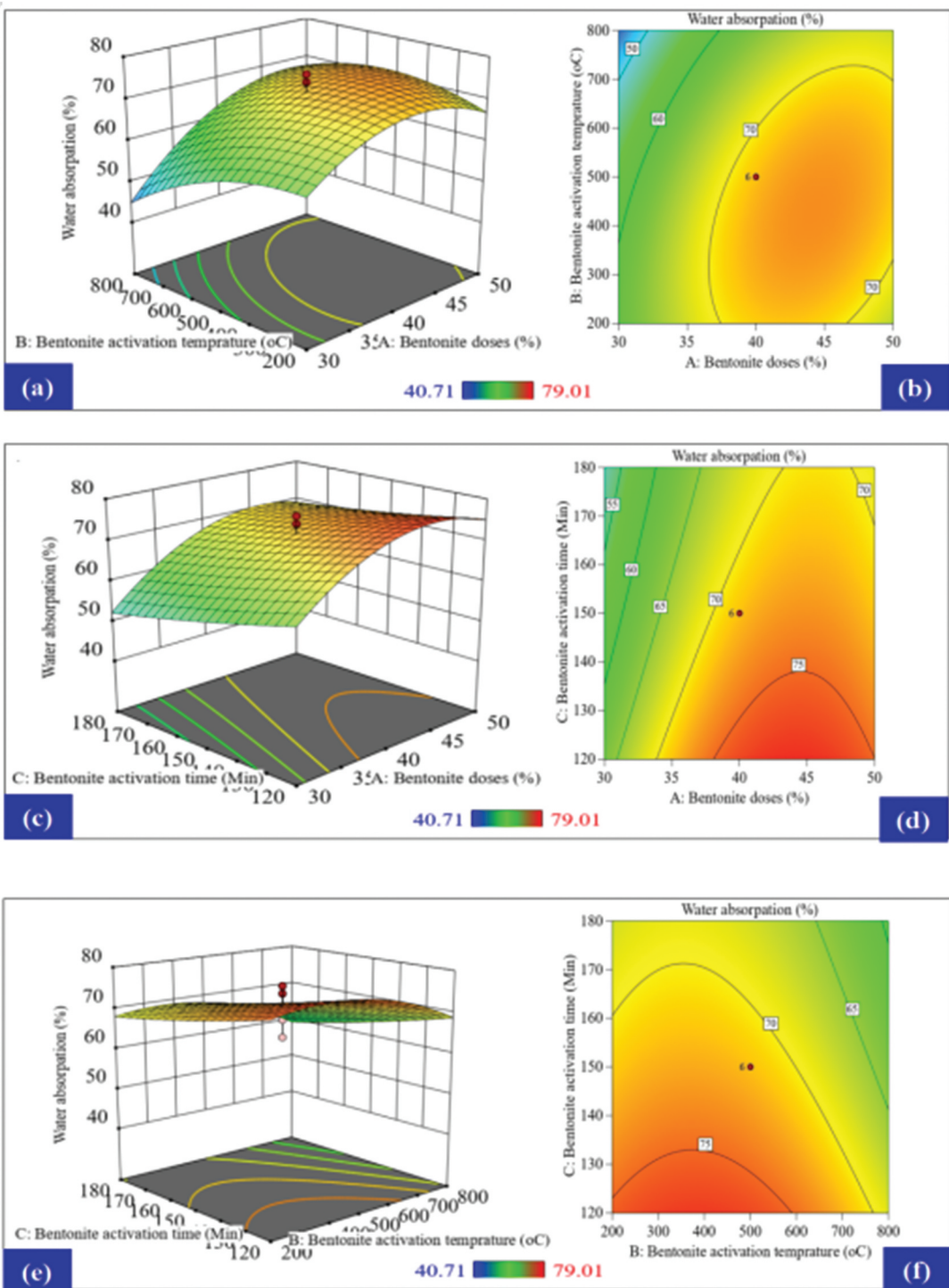


Figure 7. Interaction of treated sisal fiber water absorption with different factors by 3D and contour plots.

absorption of the treated sisal fiber significantly reduces with increasing calcination temperature and with 30–35% bentonite replacement. Especially, the lowest water absorption of around 40% is achieved when sisal is treated with a slurry prepared using 30% calcined bentonite replacement heated at 800°C, which is highly confirmed with the point of higher degradation resistance of the treated sisal fiber. This is mainly because, at 800°C, bentonite reaches the highest reactivity with free lime in cement and produces C-H-S gel, which can create a dense structure that prevents water absorption into the sisal fiber matrix. However, at higher bentonite substitution to the binder, the water absorption is high compared to raw sisal fiber and other treated sisal fibers.

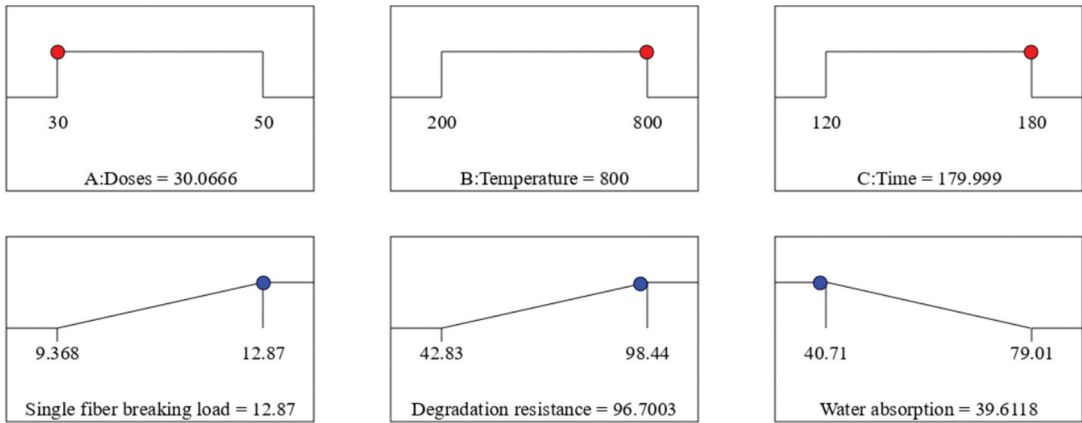
Also, as illustrated in [Figure 7\(c,d\)](#), the water absorption of the treated sisal fiber significantly reduces while increasing the calcination time of bentonite used for treating sisal fiber; however, higher sisal fiber water absorption, at lower bentonite calcination time and higher bentonite replacement respectively at 120 to 130 min and 40 to 50%. This is because, at lower calcination times and higher bentonite replacement doses, the pozzolanic reactivity of the bentonite with cement is low, which cannot promise the protection of water absorption resistance and mineralization of free lime in sisal fiber. Furthermore, as shown in [Figure 7\(e,f\)](#), the water absorption of the treated sisal fiber increases with decreasing calcination time and temperature. Especially, it exhibits the highest water absorption at 120 min and temperatures below 600°C, which are the calcination time and temperature of the calcined bentonite used for sisal fiber treatment. However, increasing bentonite calcination time and temperature from 120 to 180 min and 600 to 800°C significantly reduces the water absorption of the calcined bentonite-coated sisal fiber. Especially, at a calcination temperature of 800°C and time above 130 min, there is a significant reduction in the water absorption of treated sisal fiber, and the lowest water absorption is recorded for sisal fiber treated with calcined bentonite at 800°C for 180 min. This observation is similar to that obtained by De Filho, De Andrade Silva, and Dias Toledo Filho (2013), who found that the pores of the sisal fiber lead to higher water absorption, which attributes for degradation. Additionally, calcium hydroxide in cement is another reason for sisal fiber mineralization and consequent higher degradation. Therefore, the highly reactive calcined bentonite has the potential to react with free calcium hydroxide and fill the pores of sisal fiber, which helps reduce water absorption and enhance degradation resistance.

Sisal fiber treatment numerical optimization

Using CCD-RSM numerical optimization, the pozzolanic treatment of sisal fiber aging in cement composite material is conducted based on the specified goals presented in [Table 9](#). These goals include maximizing the breaking load and degradation resistance with minimizing water absorption of sisal fiber by assessing different methods of sisal fiber treatment through calcined bentonite slurry prepared with a calcination temperature of 200– 800°C, a calcination time of 180 min, and a dosage of 30–50%. However, CCD-RSM is able to evaluate the effect of those factors out of the lower and higher recorded limits. So, based on the established goals, 43 optimized values are generated, and the first optimum values selected are a calcined bentonite dosage of 30.067%, a calcination temperature of 800°C, and a calcination time of 179.99 min, which can yield a sisal fiber breaking load of 12.87 N, degradation resistance of 96.70%, and water absorption of 39.61%, as illustrated in [Figure 8](#). This selection is based on its ability to better fulfill the established goals and achieve higher desirability, as shown in [Figure 9](#), which indicates that as desirability

Table 9. The established optimization constraints.

Name	Goal	Lower limit	Upper limit	Lower weight	Upper weight	Importance
A: Bentonite dose	Is in range	30.000	50.000	1.000	1.000	3.000
B: Calcination temperature	Is in range	200.000	800.000	1.000	1.000	3.000
C: Calcination time	Is in range	120.000	180.000	1.000	1.000	3.000
Single fiber breaking load	Maximize	9.368	12.87	1.000	1.000	3.000
Degradation resistance	Maximize	42.83	98.44	1.000	1.000	3.000
Water absorption	Minimize	40.71	39.6118	1.000	1.000	3.000



Desirability = 0.989
Solution 1 out of 43

Figure 8. Numerical optimization of treated sisal fiber by optimization ramp for all factors and responses.

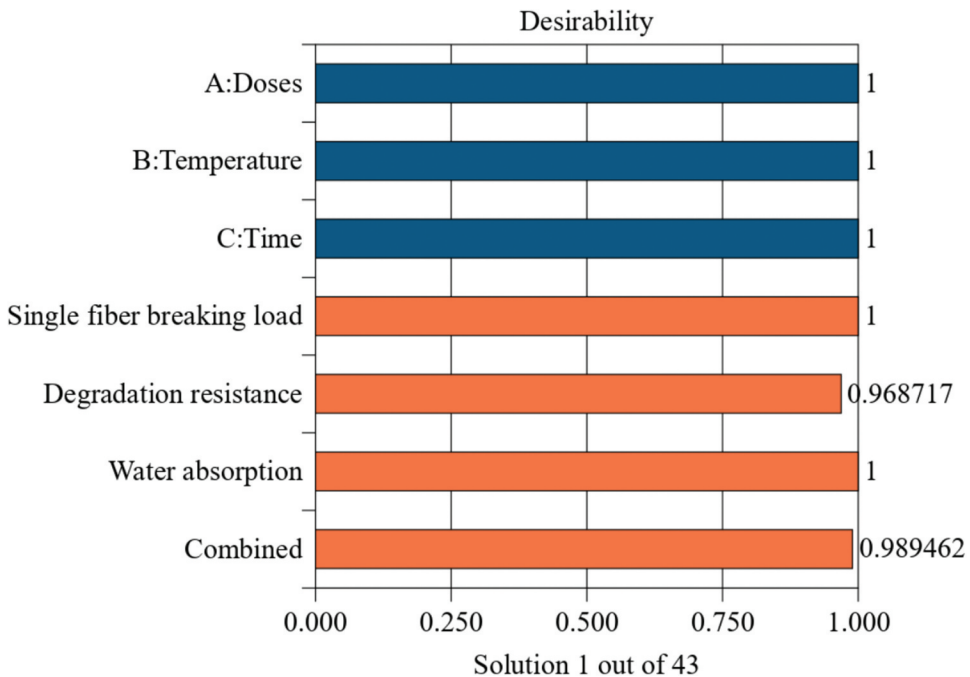


Figure 9. Desirability of the selected optimum treated sisal fiber.

approaches the unit, the reliability of the suggested numerical values to the actual experimental results increases, as noted by Myers, Montgomery, and Anderson (). The selected optimum values can effectively treat the sisal fiber because the bentonite at 800°C can be changed from a crystalline to an amorphous state, as shown in our previous study (Fode, Abeid, Jande, and Kivevele 2024), which can react with free calcium hydroxide in cement and can consequently reduce the effect of

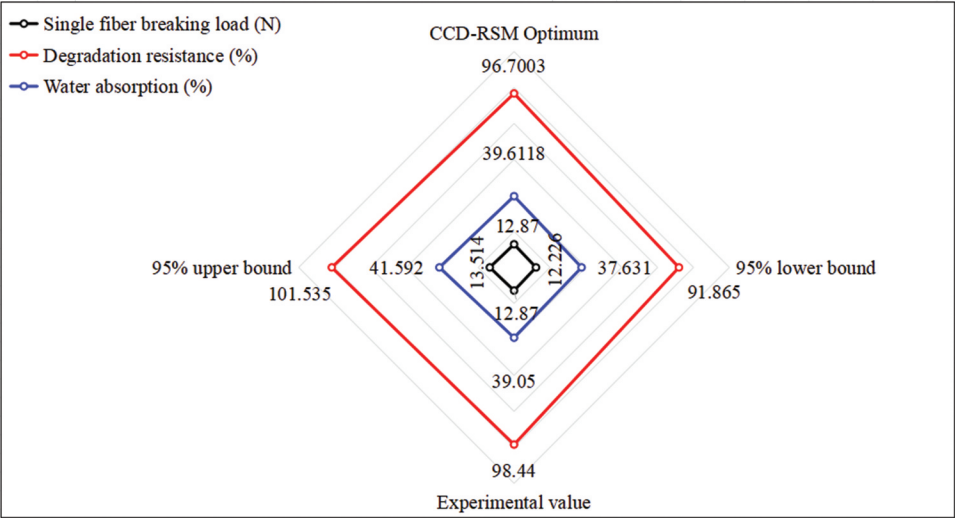


Figure 10. Experimental validation of optimized CCR-RSM values.

deterioration of sisal fiber caused by calcium hydroxide mineralization. The micro-filling ability of calcined bentonite also helps to protect the surface pores of sisal fiber from water absorption.

Sisal fiber treatment experimental validation

For all the response parameters of the sisal fiber treatment method, the optimum numerical value was validated experimentally by taking a calcined bentonite dose of 30.067%, bentonite calcination temperature of 800°C, and calcination time of 179.99 min. This is to evaluate experimentally as it can confirm the optimum numerical suggested values, breaking load 12.87 N, degradation resistance

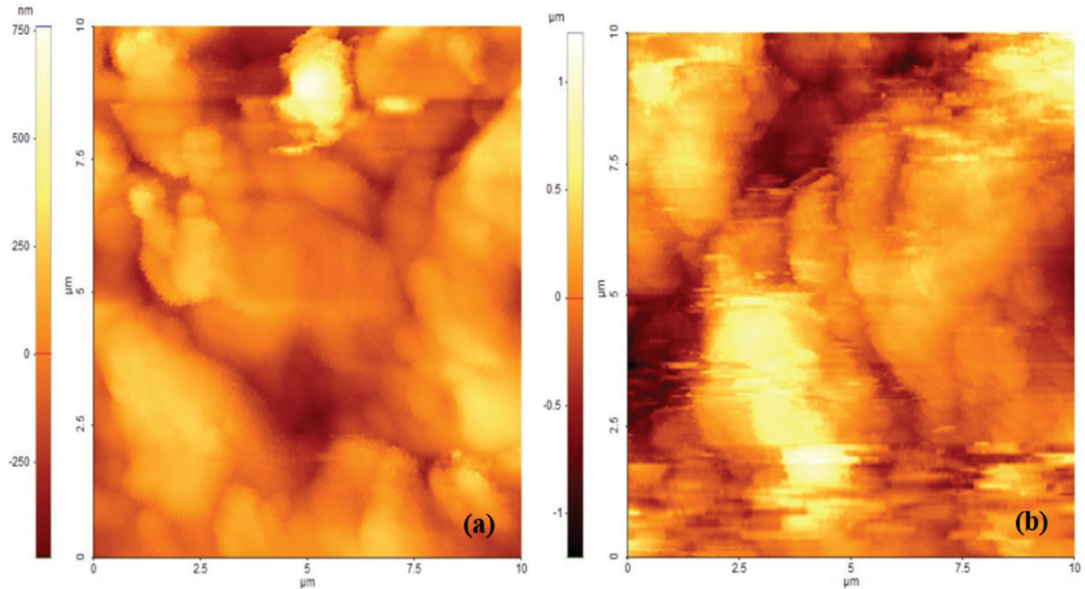


Figure 11. Atomic force microscope results: (a) raw sisal fiber and (b) optimized treated sisal fiber.

96.70%, and water absorption 39.61% or near up to $\pm 5\%$ error. The variation between the numerical and experimental values was determined as shown in Eq. 4, while the experimental data have been conducted three times, and the average is reported for all response factors.

$$\varepsilon = \frac{(\delta_1 - \delta_2)}{\delta_1} * 100 \quad (4)$$

where ε is the percentage of error, δ_1 and δ_2 are the experimental and model response values, respectively.

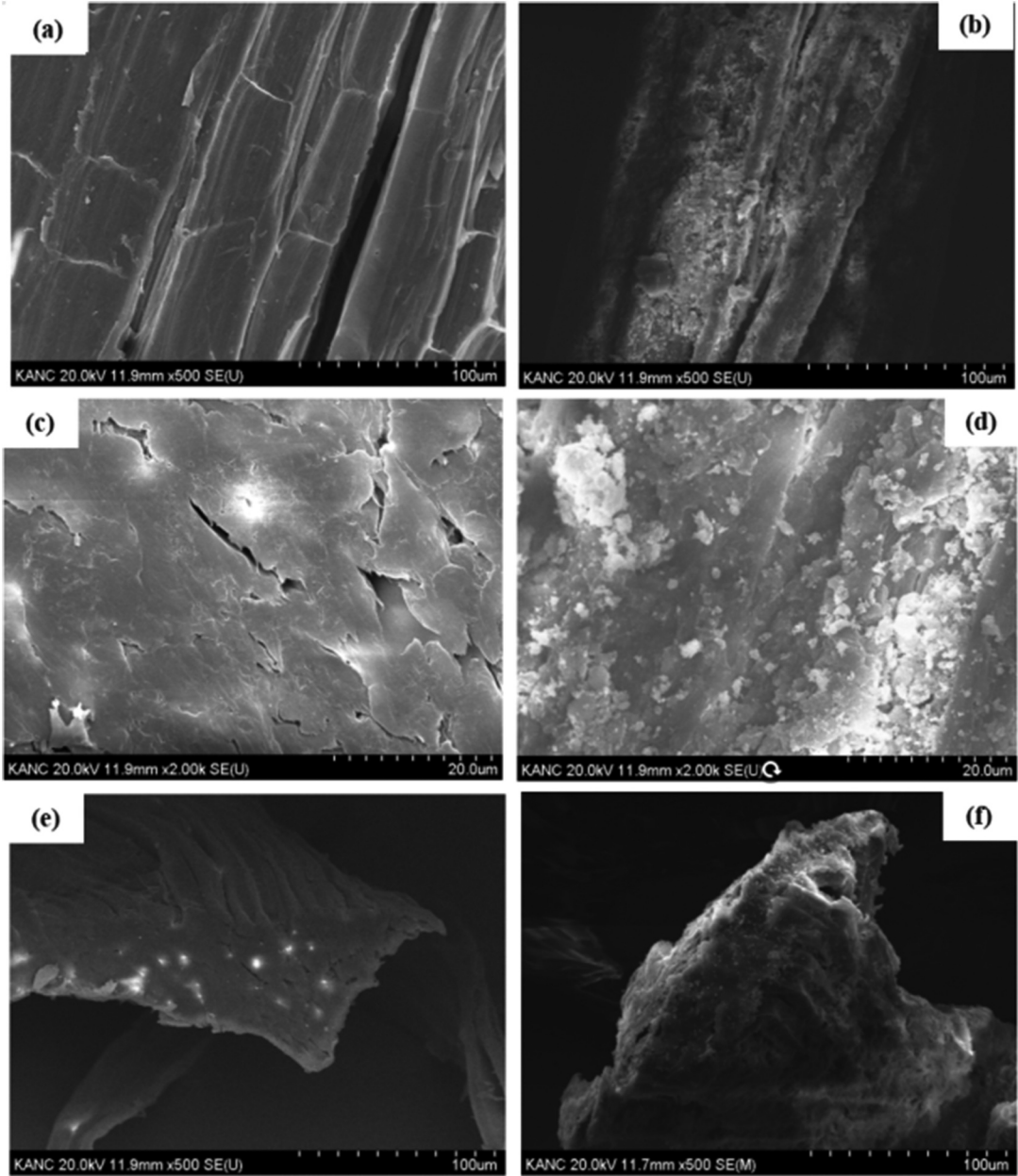


Figure 12. SEM results for raw and optimized treated sisal fibers respectively: (a,b) longitudinal direction of the fibers, (c,d) magnified longitudinal direction of the fibers, and (e,f) transversal direction of the fibers.

Using the numerically suggested factors, the experimental results are as follows: breaking load of 12.87 N, degradation resistance of 98.44%, and water absorption of 39.05%. As presented in [Figure 10](#), the variation between the numerical optimum values and the experimental results is within the acceptable 95% confidence level, which means that all the response errors between the numerically suggested and experimental values are within $\pm 5\%$, having 0%, +1.799%, and -0.1738% for breaking load, degradation resistance, and water absorption, respectively. Hence, this indicates that the CCD-RSM-suggested quadratic model for sisal fiber treatment by calcined bentonite slurry is accurate and reliable.

Surface roughness

Sisal fiber roughness is a highly influencing property that can determine the bond between the fiber and the matrix of cement composite materials. [Figure 11](#) shows the atomic force microscope results indicating that the surface roughness of the raw sisal fiber varies from +750 to -250 nm, while the surface roughness of the optimized treated sisal fiber varies from +1000 to -1000 nm, indicating that the treated sisal fiber has a significantly higher surface roughness than the raw sisal fiber, mainly due to the coated slurry used for the treatment. Therefore, a rougher structure is crucial for strengthening the bond and adhesion of the fiber with the cement composite matrix. This observation is similar to the findings of Orue et al. (2015), which noted that the treated sisal fiber has a rougher surface compared to the raw sisal fiber.

Microstructure

The result in [Figure 12](#) shows the microstructure of raw and optimized treated sisal fiber in longitudinal and transversal directions. As shown in [Figure 12\(a,b\)](#), the surface of the treated sisal fiber is coated with calcined bentonite slurry. In [Figure 12\(c,d\)](#), the magnified result indicates that the raw sisal fiber has pores on the surface that can absorb water, which can lead to the degradation of sisal fiber in the cement composite materials. However, the surface of the optimized sisal fiber shows no pores, as the treatment with calcined bentonite slurry fills the pores, creating a barrier against moisture and cement mineralization, which can allow to resist the degradation of the sisal fiber. Additionally, [Figure 12\(d,e\)](#) illustrates the transversal way of sisal fiber microstructure, which shows that the raw sisal fiber has pores, and the treated sisal fibers have been coated with calcined bentonite slurry treatment.

Conclusions

The present study modeled and optimized the treatment method of sisal fiber degradation using different calcined bentonite slurries for cement composite materials using the central composite design-response surface method. Key parameters considered included single fiber breaking load, sisal fiber degradation resistance, and water absorption. The following conclusions have been reached.

- Increasing the calcination temperature and replacement dose of bentonite used for sisal fiber treatment highly increases the sisal fiber tensile strength and breaking load. Especially, the highest breaking load was achieved for coated sisal fiber treated with a 40–45% bentonite dose replacement in cement at 800°C calcination of bentonite. At bentonite calcination temperature and calcination time, respectively 200°C and 180 min or 800°C and 120 min, the breaking load of the treated sisal fiber is lower compared to other treated sisal fibers.
- The degradation resistance of sisal fiber increases with increasing calcination temperature and time of calcined bentonite. Also, the treated sisal fiber reached a higher aging resistance at calcination time 150–180 min and 600–800°C calcination temperature of bentonite.

- The lowest water absorption is recorded for sisal fiber treated with calcined bentonite at a 30–35% replacement dose, which calcined at 800°C for 180 min.
- The optimum treated sisal fiber, as predicted by CCD-RSM, was achieved with a calcined bentonite dose of 30.067%, a calcination temperature of 800°C, and a calcination time of 179.99 min. Experimentally, those numerical factors of treated sisal fiber validated which gave a breaking load of 12.87 N, degradation resistance of 98.44%, and water absorption of 39.05%, all confirmed within a 95% confidence level.
- The optimum treated sisal fiber improved breaking load by 33.37% and degradation resistance by 98% while reducing water absorption by 60.95% compared to the raw sisal fiber.
- The optimum treated sisal fiber has a higher surface roughness compared to the raw sisal fiber. However, the raw sisal fiber has a higher surface pore than the optimum treated sisal fiber.

Highlights

- Sisal fiber treatment with calcined bentonite effectively improves sisal fiber degradation resistance for cement composite materials.
- Sisal fiber treated with calcined bentonite has higher surface roughness and lower pores than raw sisal fiber.
- Sisal fiber treated with calcined bentonite reduces the water absorption of the fiber.

Acknowledgments

The authors greatly appreciate the Partnership for Applied Sciences, Engineering, and Technology (PASET) – Regional Scholarship and Innovation Fund (RSIF) for the support of this study.

Nomenclatures

ANOVA	Analysis Of Variance
CCD-RSM	Central Composite Design-Response Surface Method
C-H-S	Calcium Hydrate Sulfate
DEFIT	Difference in fits
LOF	Lack Of Fit

Disclosure statement

No potential conflict of interest was reported by the author(s).

ORCID

Tsion Amsalu Fode  <http://orcid.org/0000-0002-9186-6517>

References

- Abbass, W., M. I. Khan, and S. Mourad. 2018. "Evaluation of Mechanical Properties of Steel Fiber Reinforced Concrete with Different Strengths of Concrete." *Construction and Building Materials* 168:556–569. <https://doi.org/10.1016/j.conbuildmat.2018.02.164>.
- Abirami, R., and S. P. Sangeetha. 2022. "Effect of Surface Modification on the Characteristics of Sisal Fiber Reinforced Concrete Treated with Na₂CO₃." *Nature Environment & Pollution Technology* 21 (1): 289–295. <https://doi.org/10.46488/NEPT.2022.v21i01.034>.
- Afolayan, J. O., U. N. Wilson, and B. Zaphaniah. 2019. "Effect of Sisal Fibre on Partially Replaced Cement with Periwinkles Shell Ash (PSA) Concrete." *Journal of Applied Sciences and Environmental Management* 23 (4): 715. <https://doi.org/10.4314/jasem.v23i4.22>.

- Ali, M. S., R. Arsalan, S. Khan, and T. Yiu Lo. 2012. "Utilization of Pakistani Bentonite as Partial Replacement of Cement in Concrete." *Construction and Building Materials* 30:237–242. <https://doi.org/10.1016/j.conbuildmat.2011.11.021>.
- Ali-Boucetta, T., A. Ayat, W. Laifa, and M. Behim. 2021. "Treatment of Date Palm Fibres Mesh: Influence on the Rheological and Mechanical Properties of Fibre-Cement Composites." *Construction and Building Materials* 273:121056. <https://doi.org/10.1016/j.conbuildmat.2020.121056>.
- Arshad, S., M. Burhan, S. Muhammad, H. Mehran, K. Jiao, and L. Zhang. 2020. "Efficiency of Supplementary Cementitious Materials and Natural Fiber on Mechanical Performance of Concrete." *Arabian Journal for Science & Engineering* 45 (10): 8577–8589. <https://doi.org/10.1007/s13369-020-04769-z>.
- Asim, M., G. Moeen Uddin, H. Jamshaid, A. Raza, Z. Ul Rehman, U. Hussain, A. Naseem Satti, N. Hayat, and S. Muhammad Arafat. 2020. "Comparative Experimental Investigation of Natural Fibers Reinforced Light Weight Concrete as Thermally Efficient Building Materials." *Journal of Building Engineering* 31 (August 2019): 101411. <https://doi.org/10.1016/j.jobbe.2020.101411>.
- Belaadi, A., A. Bezazi, M. Bouchak, and F. Scarpa. 2013. "Tensile Static and Fatigue Behaviour of Sisal Fibres." *Materials & Design* 46:76–83. <https://doi.org/10.1016/j.matdes.2012.09.048>.
- Belaadi, A., M. Boumaaza, H. Alshahrani, M. Bouchak, and H. Satha. 2023. "Improving the Mechanical Performance of Biocomposite Plaster/Washingtonia Filifera: Optimization Comparison Between ANN and RSM Approaches." *Journal of Natural Fibers* 20 (1). <https://doi.org/10.1080/15440478.2023.2170945>.
- Benítez-Guerrero, M., L. A. Pérez-Maqueda, R. Artiaga, P. E. Sánchez-Jiménez, and J. Pascual-Cosp. 2017. "Structural and Chemical Characteristics of Sisal Fiber and Its Components: Effect of Washing and Grinding." *Journal of Natural Fibers* 14 (1): 26–39. <https://doi.org/10.1080/15440478.2015.1137529>.
- Bolat, H., Ö. Şimşek, M. Çullu, G. Durmuş, and Ö. Can. 2014. "The Effects of Macro Synthetic Fiber Reinforcement Use on Physical and Mechanical Properties of Concrete." *Composites Part B Engineering* 61:191–198. <https://doi.org/10.1016/j.compositesb.2014.01.043>.
- Boudermine, H., M. Boumaaza, A. Belaadi, M. Bouchak, and M. Bencheikh. 2024. "Performance Analysis of Biochar and W. Robusta Palm Waste Reinforced Green Mortar Using Response Surface Methodology and Machine Learning Methods." *Construction and Building Materials* 438:137214. <https://doi.org/10.1016/j.conbuildmat.2024.137214>.
- Cinku, K., F. Karakas, and F. Boylu. 2014. "Effect of Calcinated Magnesite on Rheology of Bentonite Suspensions. Magnesia-Bentonite Interaction." *Physicochemical Problems of Mineral Processing* 50 (2): 453–466. <https://doi.org/10.5277/ppmp140203>.
- Dahish, H. A., and A. D. Almutairi. 2023. "Effect of Elevated Temperatures on the Compressive Strength of Nano-Silica and Nano-Clay Modified Concretes Using Response Surface Methodology." *Case Studies in Construction Materials* 18 (January): e02032. <https://doi.org/10.1016/j.cscm.2023.e02032>.
- De Filho, J. A. M., F. De Andrade Silva, and R. Dias Toledo Filho. 2013. "Degradation Kinetics and Aging Mechanisms on Sisal Fiber Cement Composite Systems." *Cement and Concrete Composites* 40:30–39. <https://doi.org/10.1016/j.cemconcomp.2013.04.003>.
- de Lima, T. E. S., A. R. G. de Azevedo, M. T. Marvila, V. S. Candido, R. Fediuk, and S. N. Monteiro. 2022. "Potential of Using Amazon Natural Fibers to Reinforce Cementitious Composites: A Review." *Polymers* 14 (3): 1–20. <https://doi.org/10.3390/polym14030647>.
- de Souza Castoldi, R., L. M. S. de Souza, and F. de Andrade Silva. 2019. "Comparative Study on the Mechanical Behavior and Durability of Polypropylene and Sisal Fiber Reinforced Concretes." *Construction and Building Materials* 211:617–628. <https://doi.org/10.1016/j.conbuildmat.2019.03.282>.
- Ferreira, D. P., J. Cruz, and R. Figueiro. 2018. "Surface Modification of Natural Fibers in Polymer Composites." In *Green Composites for Automotive Applications*, 3–41. Elsevier Ltd. <https://doi.org/10.1016/B978-0-08-102177-4.00001-X>.
- Ferreira, S. R., F. de Andrade Silva, P. Roberto Lopes Lima, and R. Dias Toledo Filho. 2017. "Effect of Hornification on the Structure, Tensile Behavior and Fiber Matrix Bond of Sisal, Jute and Curauá Fiber Cement Based Composite Systems." *Construction and Building Materials* 139:551–561. <https://doi.org/10.1016/j.conbuildmat.2016.10.004>.
- Ferreira, S. R., P. R. L. Lima, F. A. Silva, and R. D. Toledo Filho. 2014. "Effect of Sisal Fiber Hornification on the Fiber-Matrix Bonding Characteristics and Bending Behavior of Cement Based Composites." *Key Engineering Materials* 600:421–432. <https://doi.org/10.4028/www.scientific.net/KEM.600.421>.
- Fidelis, M. E. A., R. Dias Toledo Filho, F. de Andrade Silva, V. Mechtcherine, M. Butler, and S. Hempel. 2016. "The Effect of Accelerated Aging on the Interface of Jute Textile Reinforced Concrete." *Cement and Concrete Composites* 74:7–15. <https://doi.org/10.1016/j.cemconcomp.2016.09.002>.
- Fode, T. A., Y. Abeid, C. Jande, and T. Kivevele. 2024. "Effects of Raw and Different Calcined Bentonite on Durability and Mechanical Properties of Cement Composite Material." *Case Studies in Construction Materials* 20 (e03012): 1–17. <https://doi.org/10.1016/j.cscm.2024.e03012>.
- Fode, T., Y. Abeid, C. Jande, T. Kivevele, T. A. Fode, and T. Kivevele. 2024. "A Review on Degradation Improvement of Sisal Fiber by Alkali and Pozzolana for Cement Composite Materials." *Journal of Natural Fibers* 21 (1): 1. <https://doi.org/10.1080/15440478.2024.2335327>.

- Fode, T. A., Y. Jande, C. Abeid, and T. Kivevele. 2024. "Modelling and Optimization of Multiple Replacement of Supplementary Cementitious Materials for Cement Composite by Response Surface Method." *Cleaner Engineering and Technology* 19 (100735): 1–18. <https://doi.org/10.1016/j.clet.2024.100735>.
- Gao, C., Q. Fu, L. Huang, L. Yan, and G. Gu. 2022. "Jute Fiber-Reinforced Polymer Tube-Confined Sisal Fiber-Reinforced Recycled Aggregate Concrete Waste." *Polymers* 14 (6): 1260. <https://doi.org/10.3390/polym14061260>.
- Gonzalez-Lopez, L., J. Claramunt, Y. Lo Hsieh, H. Ventura, and M. Ardanuy. 2020. "Surface Modification of Flax Nonwovens for the Development of Sustainable, High Performance, and Durable Calcium Aluminate Cement Composites." *Composites Part B Engineering* 191 (March): 107955. <https://doi.org/10.1016/j.compositesb.2020.107955>.
- Gupta, U. S., M. Dhamarikar, A. Dharkar, S. Chaturvedi, S. Tiwari, and R. Namdeo. 2020. "Surface Modification of Banana Fiber: A Review." *Materials Today: Proceedings* 43 (xxxx): 904–915. <https://doi.org/10.1016/j.matpr.2020.07.217>.
- Hanif, I. M., M. R. Noor Syuhaili, M. F. Hasmori, and S. M. Shahmi. 2017. "Effect of Nylon Fiber on Mechanical Properties of Cement Based Mortar." *IOP Conference Series: Materials Science & Engineering* 271 (1): 012080. <https://doi.org/10.1088/1757-899X/271/1/012080>.
- Hasan, R., M. H. R. Sobuz, A. S. M. Akid, M. R. Awall, M. Houda, A. Saha, M. M. Meraz, M. S. Islam, and N. M. Sutan. 2023. "Eco-Friendly Self-Consolidating Concrete Production with Reinforcing Jute Fiber." *Journal of Building Engineering* 63 (PA): 105519. <https://doi.org/10.1016/j.job.2022.105519>.
- Herrera-Franco, P. J., J. G. Carrillo, and Q. M. Li. 2020. "Mechanical Properties of Natural Fiber Reinforced Foamed Concrete." *Materiale MDPI* 13 (14): 1–18. <https://doi.org/10.3390/ma13143060>.
- Iniya, M. P., and K. Nirmalkumar. 2021. "A Review on Fiber Reinforced Concrete Using Sisal Fiber." *IOP Conference Series: Materials Science & Engineering* 1055 (1): 012027. <https://doi.org/10.1088/1757-899x/1055/1/012027>.
- Izquierdo, I. S., O. S. Izquierdo, M. A. Ramalho, and A. Taliércio. 2017. "Sisal Fiber Reinforced Hollow Concrete Blocks for Structural Applications: Testing and Modeling." *Construction and Building Materials* 151:98–112. <https://doi.org/10.1016/j.conbuildmat.2017.06.072>.
- Jamshaid, H., R. Kumar Mishra, A. Raza, U. Hussain, M. Lutfur Rahman, S. Nazari, V. Chandan, M. Muller, and R. Choteborsky. 2022. "Natural Cellulosic Fiber Reinforced Concrete: Influence of Fiber Type and Loading Percentage on Mechanical and Water Absorption Performance." *Materials* 15 (3): 3. <https://doi.org/10.3390/ma15030874>.
- Jeyapragash, R., V. Srinivasan, and S. Sathiyamurthy. 2020. "Mechanical Properties of Natural Fiber/Particulate Reinforced Epoxy Composites - a Review of the Literature." *Materials Today: Proceedings* 22 (xxxx): 1223–1227. <https://doi.org/10.1016/j.matpr.2019.12.146>.
- Kafodya, I., and F. Okonta. 2018. "Effects of Natural Fiber Inclusions and Pre-Compression on the Strength Properties of Lime-Fly Ash Stabilised Soil." *Construction and Building Materials* 170:737–746. <https://doi.org/10.1016/j.conbuildmat.2018.02.194>.
- Kumar, P., and R. Roy. 2018. "Study and Experimental Investigation of Flow and Flexural Properties of Natural Fiber Reinforced Self Compacting Concrete." In *Procedia Computer Science*, 598–608. Vol. 125. Elsevier B.V. <https://doi.org/10.1016/j.procs.2017.12.077>.
- Latifi, M. R., Ö. Biricik, and A. Mardani Aghabaglou. 2022. "Effect of the Addition of Polypropylene Fiber on Concrete Properties." *Journal of Adhesion Science and Technology* 36 (4): 345–369. <https://doi.org/10.1080/01694243.2021.1922221>.
- Machaka, M. M., H. S. Basha, and A. M. Elkordi. 2014. "The Effect of Using Fan Palm Natural Fibers on the Mechanical Properties and Durability of Concrete." *International Journal of Materials Science and Engineering* 2 (January). <https://doi.org/10.12720/ijmse.2.2.76-80>.
- Martinelli, F. R. B., F. Roger Carneiro Ribeiro, M. Teixeira Marvila, S. Neves Monteiro, F. da Costa Garcia Filho, and A. R. G. de Azevedo. 2023. "A Review of the Use of Coconut Fiber in Cement Composites." *Polymers* 15 (5): 1–15. <https://doi.org/10.3390/polym15051309>.
- Marvila, M. T., H. Azevedo Rocha, A. R. G. de Azevedo, H. A. Colorado, J. F. Zapata, and C. Mauricio Fontes Vieira. 2021. "Use of Natural Vegetable Fibers in Cementitious Composites: Concepts and Applications." *Innovative Infrastructure Solutions* 6 (3): 1–24. <https://doi.org/10.1007/s41062-021-00551-8>.
- Messaouda, B., A. Belaadi, H. Alshahrani, K. A. K. Mohammad, and M. Jawaid. 2023. "Environmentally Mortar Development Using Washingtonia/Biochar Waste Hybrid: Mechanical and Thermal Properties." *Biomass Conversion and Biorefinery*. <https://doi.org/10.1007/s13399-023-04743-3>.
- Mohammed, B. S., S. Haruna, M. M. B. A. Wahab, and M. S. Liew. 2019. "Optimization and Characterization of Cast in-Situ Alkali-Activated Pastes by Response Surface Methodology." *Construction and Building Materials* 225:776–787. <https://doi.org/10.1016/j.conbuildmat.2019.07.267>.
- Mudadu, A., G. Tiberti, F. Germano, G. A. Plizzari, and A. Morbi. 2018. "The Effect of Fiber Orientation on the Post-Cracking Behavior of Steel Fiber Reinforced Concrete Under Bending and Uniaxial Tensile Tests." *Cement and Concrete Composites* 93:274–288. <https://doi.org/10.1016/j.cemconcomp.2018.07.012>.

- Naraganti, S. R., R. Mohan Rao Pannem, and J. Putta. 2019. "Impact Resistance of Hybrid Fibre Reinforced Concrete Containing Sisal Fibres." *Ain Shams Engineering Journal* 10 (2): 297–305. <https://doi.org/10.1016/j.asej.2018.12.004>.
- Naveen, J., M. Jawaid, P. Amuthakkannan, and M. Chandrasekar. 2018. "Mechanical and Physical Properties of Sisal and Hybrid Sisal Fiber-Reinforced Polymer Composites." In *Mechanical and Physical Testing of Biocomposites, Fibre-Reinforced Composites and Hybrid Composites*, 427–440. Elsevier Ltd. <https://doi.org/10.1016/B978-0-08-102292-4.00021-7>.
- Orue, A., A. Jauregi, C. Peña-Rodriguez, J. Labidi, A. Eceiza, and A. Arbelaiz. 2015. "The Effect of Surface Modifications on Sisal Fiber Properties and Sisal/Poly (Lactic Acid) Interface Adhesion." *Composites Part B Engineering* 73:132–138. <https://doi.org/10.1016/j.compositesb.2014.12.022>.
- Ramesh, M. 2018. "Hemp, Jute, Banana, Kenaf, Ramie, Sisal Fibers." In *Handbook of Properties of Textile and Technical Fibres*, 301–325. Elsevier Ltd. <https://doi.org/10.1016/B978-0-08-101272-7.00009-2>.
- Reddy, S. S., and M. Achyutha Kumar Reddy. 2021. "Optimization of Calcined Bentonite Caly Utilization in Cement Mortar Using Response Surface Methodology." *International Journal of Engineering, TRANSACTIONS A: Basics* 34 (7): 1623–1631. <https://doi.org/10.5829/IJE.2021.34.07A.07>.
- Shadheer Ahamed, M., P. Ravichandran, and A. R. Krishnaraja. 2021. "Natural Fibers in Concrete – a Review." *IOP Conference Series: Materials Science & Engineering* 1055 (1): 012038. <https://doi.org/10.1088/1757-899x/1055/1/012038>.
- Shadrach Jeya Sekaran, A., K. Palani Kumar, and K. Pitchandi. 2015. "Evaluation on Mechanical Properties of Woven Aloe vera and Sisal Fibre Hybrid Reinforced Epoxy Composites." *Bulletin of Materials Science* 38 (5): 1183–1193. <https://doi.org/10.1007/s12034-015-0999-4>.
- Singh, S., M. Iqbal Khairandish, M. Musleh Razahi, R. Kumar, J. Singh Chohan, A. Tiwary, S. Sharma, et al. 2022. "Preference Index of Sustainable Natural Fibers in Stone Matrix Asphalt Mixture Using Waste Marble." *Materials* 15 (8): 1–17. <https://doi.org/10.3390/ma15082729>.
- Thomas, B. C., and Y. Stalin Jose. 2022. "Impact of Sisal Fiber Reinforced Concrete and Its Performance Analysis: A Review Biju." *Evolutionary Intelligence* 15 (2): 865–875. <https://doi.org/10.1007/s12065-019-00230-9>.
- Tian, H., Y. X. Zhang, C. Yang, and Y. Ding. 2015. "Recent Advances in Experimental Study on Mechanical Behaviour of Natural Fibre Reinforced Cementitious Composites." *Structural Concrete*: 1–51. <https://doi.org/10.1002/suco.201500177>.
- Vijayan, R., and A. Krishnamoorthy. 2019. "Review on Natural Fiber Reinforced Composites." In *Materials Today: Proceedings*, 897–906 16. <https://doi.org/10.1016/j.matpr.2019.05.175>.
- Wei, J., and C. Meyer. 2014a. "Sisal Fiber-Reinforced Cement Composite with Portland Cement Substitution by a Combination of Metakaolin and Nanoclay." *Journal of Materials Science* 49 (21): 7604–7619. <https://doi.org/10.1007/s10853-014-8469-8>.
- Wei, J., and C. Meyer. 2014b. "Degradation Rate of Natural Fiber in Cement Composites Exposed to Various Accelerated Aging Environment Conditions." *Corrosion Science* 88:118–132. <https://doi.org/10.1016/j.corsci.2014.07.029>.
- Wei, J., and Meyer C. 2017. "Degradation of Natural Fiber in Ternary Blended Cement Composites Containing Metakaolin and Montmorillonite." *Corrosion Science* 120:42–60. <https://doi.org/10.1016/j.corsci.2016.12.004>.
- Wu, Z., C. Shi, W. He, and L. Wu. 2016. "Effects of Steel Fiber Content and Shape on Mechanical Properties of Ultra High Performance Concrete." *Construction and Building Materials* 103:8–14. <https://doi.org/10.1016/j.conbuildmat.2015.11.028>.
- Yadav, D., G. R. Selokar, A. Agrawal, V. Mishra, and I. A. Khan. 2021. "Effect of Concentration of NaOH Treatment on Mechanical Properties of Epoxy/Sisal Fiber Composites." *IOP Conference Series: Materials Science & Engineering* 1017 (1): 012028. <https://doi.org/10.1088/1757-899X/1017/1/012028>.
- Zakaria, M., M. Ahmed, M. M. Hoque, and S. Islam. 2017. "Scope of Using Jute Fiber for the Reinforcement of Concrete Material." *Textiles and Clothing Sustainability* 2 (1). <https://doi.org/10.1186/s40689-016-0022-5>.
- Zhang, P., S. Han, S. Ng, and X. Hao Wang. 2018. "Fiber-Reinforced Concrete with Application in Civil Engineering." *Advances in Civil Engineering* 2018 (1). <https://doi.org/10.1155/2018/1698905>.
- Zhou, X., H. Saini, and G. Kastiukas. 2017. "Engineering Properties of Treated Natural Hemp Fiber-Reinforced Concrete." *Frontiers in Built Environment* 3 (June): 1–9. <https://doi.org/10.3389/fbuil.2017.00033>.